◆ Human Brain Mapping 16:92–103(2002) ◆
DOI 10.1002/hbm.10030

Sensory System Interactions During Simultaneous Vestibular and Visual Stimulation in PET

Angela Deutschländer,[1]* Sandra Bense,[2] Thomas Stephan,[1] Markus Schwaiger,[3] Thomas Brandt,[1] and Marianne Dieterich[2]

[1]*Department of Neurology, Klinikum Grosshadern, Ludwig-Maximilians University, Munich, Germany*
[2]*Department of Neurology, Johannes Gutenberg University, Mainz, Germany*
[3]*Department of Neuroradiology, Technical University, Munich, Germany*

Abstract: The patterns of regional cerebral blood flow (rCBF) increases and decreases in PET were compared for unimodal vestibular, unimodal visual, and for simultaneous vestibular and visual stimulation. Thirteen healthy volunteers were exposed to a) caloric vestibular stimulation, b) small-field visual motion stimulation in roll, c) simultaneous caloric vestibular and visual pattern stimulation. Unimodal vestibular stimulation led to activations of vestibular cortex areas, in particular the parieto-insular vestibular cortex (PIVC), and concurrent deactivations of visual cortical areas [Brodmann area (BA) 17–19]. Unimodal visual motion stimulation led to activations of the striate visual cortex and the motion-sensitive area in the middle temporal/middle occipital gyri (BA 19/37) with concurrent deactivations in the PIVC. Simultaneous bimodal stimulation resulted in activations of the cortical representation of both sensory modalities. In the latter condition activations and deactivations were significantly smaller compared to unimodal stimulation. The findings are consistent with the concept of an inhibitory reciprocal vestibulo-visual interaction in all three stimulus conditions. *Hum. Brain Mapping 16:92–103, 2002.* © 2002 Wiley-Liss, Inc.

Key words: deactivation; insula; multisensory; inhibition; caloric; humans

INTRODUCTION

Brain activation studies using vestibular stimulation have shown activations of the posterior insula and retroinsular regions, temporo-parietal cortex, basal ganglia, thalamus, and anterior cingulate gyrus [caloric stimulation, PET: Bottini et al., 1994, 2001; Dieterich et al., 1999; galvanic stimulation, fMRI: Bense et al., 2001; Bucher et al., 1998; Lobel et al., 1998]. The posterior insula and retroinsular regions represent the human homologue of the multisensory parieto-insular vestibular cortex (PIVC) of the monkey [Grüsser et al., 1990a,b; Guldin and Grüsser, 1996]. A second observation of brain activation studies was a simultaneous significant bilateral regional cerebral blood flow (rCBF) decrease in visual cortex areas (Brodmann area [BA] 17–19) during caloric vestibular irrigation [PET: Wenzel et al., 1996]. This was also evident as blood oxygenation level dependent (BOLD) signal decreases

Contract grant sponsor: Deutsche Forschungsgemeinschaft (Klinische Forschergruppe); Contract grant sponsor: BR 639/5-3; Contract grant sponsor: Stifter Verband; Contract grant sponsor: Wilhelm-Sander-Stiftung.

*Correspondence to: Angela Deutschländer, Department of Neurology, Klinikum Grosshadern, Marchioninistr. 15, 81377 Munich, Germany.

E-mail: adeutsch@nro.med.uni-muenchen.de

Received for publication 5 September 2001; accepted 7 December 2001

during galvanic vestibular stimulation [fMRI: Bense et al., 2001]. Visual stimulation led to an analogous distribution of visual-vestibular activations and deactivations. Large-field visual motion stimulation, which induces the sensation of self-motion, not only elicited bilateral activations of several visual cortex areas but simultaneously caused bilateral rCBF decreases of the PIVC [PET: Brandt et al., 1998]. We interpreted these findings with vestibular and visual motion stimulation to indicate a reciprocally inhibitory visual-vestibular interaction. Stimulation of one sensory system results in signal increases in the cortical representation of this sensory system and concurrent signal decreases in the other system.

The aim of this study was to compare the pattern of rCBF increases and decreases in the same subject during caloric vestibular stimulation (vestibulo-visual interaction), visual stimulation (visual-vestibular interaction), and simultaneous stimulation of both sensory systems. We were particularly interested in the activation pattern during simultaneous visual and vestibular stimulation, which provided contradictory sensory input as to the perception of motion.

MATERIALS AND METHODS

Subjects

Thirteen healthy volunteers, between 32–63 years of age (mean age 47.3 years; 12 males, one female), without any history of cochlear, vestibular, or CNS disorders participated in the study. The laterality quotient for handedness according to the 10-item inventory of the Edinburgh test [Oldfield, 1971; Salmaso and Longoni, 1985] was +100 in nine, +40 in three, and −80 in one subject. Twelve PET scans were acquired from each of the 13 subjects. No data had to be excluded. All subjects gave their informed written consent after the nature of the experimental procedure was explained in accordance with the Declaration of Helsinki. The study was approved by the Ethics Committee of the Technical University, Munich, as well as the local radiation protection authorities.

Experimental Set-Up

During PET data acquisition (Conditions A–C) subjects lay supine with a tube in the right ear for the caloric irrigation and with their heads elevated by 30° to put the horizontal semicircular canals in an upright position. A disk (diameter: 0.4 m, field of view: ±22° in vertical and horizontal directions) covered with a random dot pattern was fixed in front of the PET scanner. The presentation included a total of 63 randomly distributed dots of the same size and a gray center. No moving objects were visible for the subjects behind or beside the disk. Horizontal eye movements during the scans were recorded binocularly with DC-electrooculography (EOG). Therefore, Ag/AgCl electrodes were placed at the external canthi and on the forehead.

Condition A: Vestibular Stimulation

Subjects lay supine with eyes closed, while a caloric irrigation of the right ear was performed with 100 ml of water at 44°C for 50 sec.

Condition B: Visual Stimulation

Subjects looked at the disk, that rotated counterclockwise from the subject's viewpoint at an angular velocity of 180°/sec. Subjects were instructed to look at the gray center of the disk during the stimulus presentation without fixating any individual dots. This small-field visual motion stimulation did not induce any apparent self-motion perception (circularvection, CV) in any subject.

Condition C: Simultaneous Vestibular and Visual Stimulation

Caloric irrigation of the right ear with 100 ml of water at 44°C was performed for 50 sec, while subjects looked at the disk also used for unimodal visual motion stimulation (Condition B), which was stationary.

Condition D: Baseline Condition

During the rest condition subjects lay supine without vestibular stimulation and with eyes closed.

PET: Scanning and Data Acquisition

Measurements of the regional distribution of radioactivity were performed with a Siemens/ECAT EXACT HR+ PET scanner (CTI, Knoxville, TN) operated in 3D mode with a total axial field of view of 15.28 cm and no interplane dead space. A total of 63 slices covering the whole brain and the cerebellum were acquired per subject. Subjects heads were placed in a head holder with line markings drawn on their orbitomeatal lines and foreheads. These lines were aligned with two perpendicular lasers located at the gantry, and subject position was verified before each scan. Before collecting activation data, individual transmis-

sion scans were acquired using an external $^{68}Ge/^{68}Ga$ ring source to correct for the attenuation from skull and brain. Twelve sequential rCBF PET image sets were obtained for each subject under the Conditions A–D. Each condition was presented three times in random order. The caloric irrigation lasted for 50 sec and was completed about 20 sec before the onset of the scanning period, so that acoustic and somatosensory sensations caused by the irrigation of the external auditory canal had decayed before the scanning period began. The visual stimulation continued over the whole scanning time.

An infusion pump was used to administer a dose of 370 MBq H_2O-15 in 20 ml of normal saline solution for each of the 12 scans intravenously over 30 sec with a semi-bolus injection. Single frames were acquired for 50 sec after the tracer appeared in the brain. To allow for decay of radiation to background levels, the interval between the acquisitions was 10 minutes. Following corrections for randoms, dead time, and scatter, images were reconstructed by filtered back projection (Hanning filter, cut-off frequency 0.4 cycles per projection element) to 63 consecutive axial planes with a 128×128 matrix (voxel size $2.06 \times 2.06 \times 2.425$ mm).

Data Preprocessing

Images were analyzed on an UltraSPARC workstation (Sun Microsystems) using statistical parametric mapping (SPM99) [Friston et al., 1995a], implemented in MATLAB (Mathworks, Sherborn, MA). All volumes were realigned to the first scan of the series to correct for subject motion [Friston et al., 1995b]. An aligned set of images and a mean image were generated for each subject. In a second step, volumes were spatially normalized [Friston et al., 1995b] into the standard stereotactic space defined by the Montreal Neurological Institute (MNI) template [Friston et al., 1995b]. Resulting images contained 91 planes with voxel sizes of $2 \times 2 \times 2$ mm. Before statistical analysis, each image was smoothed with an isotropic Gaussian kernel of 12 mm (full width at half maximum) to compensate for intersubject gyral variability and to attenuate high-frequency noise, thus increasing the signal to noise ratio.

Statistical Analysis

To correct for variations in global flow across subjects and scans, an analysis of covariance (ANCOVA) was applied with global flow as the confounding variable [Friston et al., 1990, 1995a]. Subsequently, mean rCBF was scaled to an arbitrary level of 50 ml dl^{-1} min^{-1}, and these adjusted rCBF voxel values were used for further statistical analyses. Statistical parametric maps (SPM) were calculated on a voxel-by-voxel basis using the general linear model [Friston et al., 1995a] and the theory of Gaussian fields [Worsley and Friston, 1995]. Each resulting set of voxel values constitutes an SPM(t) map. Only activation and deactivation foci that were significant at a height threshold of $P < 0.001$ (uncorrected) in group analyses are reported. Uncorrected significance levels were accepted for rCBF changes in brain areas, which an a priori hypothesis based on previous PET experiments defined as activated or deactivated. We performed single-subject and group statistical comparisons. For the single-subject analyses we generated SPMs comparing the stimulation conditions with rest separately for each subject. SPMs for the group showing rCBF changes between two conditions were created by entering the results from the first level statistics into a *t*-test, according to the random effects model [Frison and Pocock, 1992; Woods et al., 1996]

Anatomical Localization

To define the anatomical sites of activation and deactivation clusters, MNI coordinates as well as defined anatomic landmarks [Naidich and Brightbill, 1996; Stephan et al., 1997; Yousry et al., 1997] and the atlas of Talairach and Tournoux [1988] were used. The insula is divided into three short (I–III) insular gyri, situated frontal to the central insular sulcus, and two long (IV–V) insular gyri, posterior to the central insular gyrus. We defined gyri I–III as anterior insula, gyri IV and V as posterior insula, and the areas posterior to gyrus V as retroinsular regions [Bense et al., 2001].

RESULTS

Vestibular Stimulation

During caloric vestibular stimulation six of the 13 subjects experienced rotatory vertigo, in two subjects vertigo was associated with mild nausea. A caloric horizontal nystagmus was recorded during the scanning phase in 11 subjects (mean slow-phase velocity of the cumulative phase: 12°/sec). The two remaining subjects exhibited no measurable nystagmus during the scanning period. The single-subject analyses revealed, that the activation and deactivation patterns of these two subjects were comparable to the patterns of the subjects with vestibular nystagmus during the scanning period.

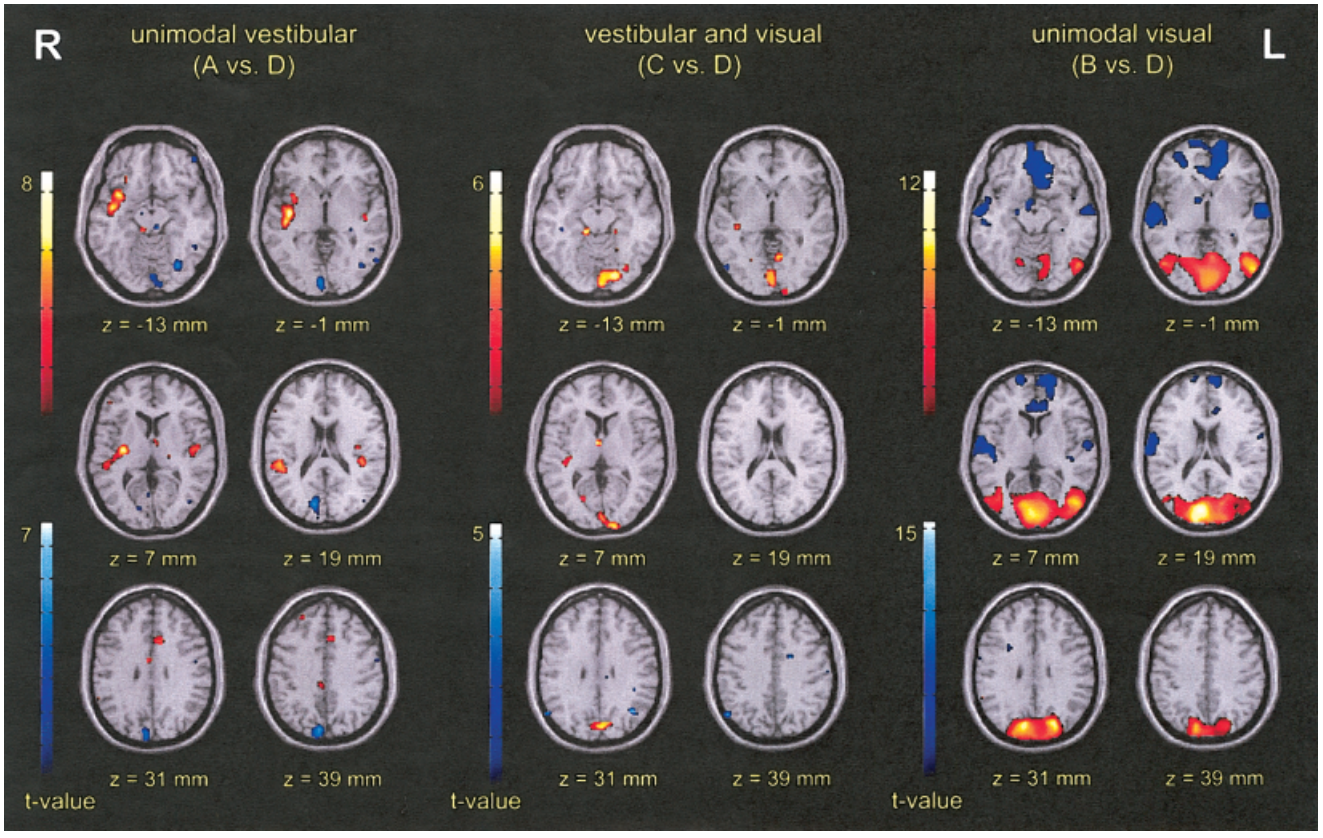

Figure 1.
Activation maps showing activations (red) and deactivations (blue) during purely vestibular (**A**), simultaneous (**B**), and purely visual (**C**) stimulation vs. rest condition (**D**) ($n = 13$; $P < 0.001$), superimposed onto the MNI standard brain template.

Activations

In the group analysis (caloric irrigation of the right ear vs. rest) bilateral activations were found in the posterior insula and adjacent retroinsular regions and in the superior temporal gyrus (BA 22). Activations were seen in two separate areas of the right insular cortex: in the short insular gyrus III (anterior insula) and the long insular gyri IV and V (posterior insula), the latter extending to Heschl gyrus and the superior and middle temporal gyri (BA 21/22/38). The left insular region showed activations of the long insular gyrus V and adjacent Heschl gyrus (Fig. 1; for *t*-values, coordinates and cluster sizes see Table I). Activations of the posterior insula or retroinsular regions were found in the single-subject analyses of all subjects ($P < 0.01$, uncorrected).

Right-sided activations were seen in the inferior parietal lobule (BA 40), posterior cingulate gyrus (BA 23, BA 31), superior temporal gyrus (BA 38), middle temporal gyrus (BA 21), and middle frontal gyrus (BA 8, BA 46). Left-sided activations were seen in the antero-medial and postero-lateral thalamus, anterior cingulate gyrus (BA 24/32), and in the cerebellar hemisphere (Fig. 1; Table I).

Activations in the globus pallidus or in the putamen appeared in single-subject analyses ($n = 7$) only ($P < 0.01$, uncorrected), whereas we found no activations in the basal ganglia in the group analysis ($P < 0.001$, uncorrected).

Deactivations

The group analysis showed bilateral deactivations of the visual cortex (middle and inferior occipital gyri, lingual gyrus [BA 17, BA 18]). Right-sided deactivations were located in the upper parts of the visual cortex (superior occipital gyrus [BA 19]), in the precuneus (BA 7), and left-sided deactivations in the middle temporal/middle occipital gyri (BA 19/37), middle/inferior frontal gyri (BA 11/47), superior/middle temporal gyri (BA 21/38), middle temporal gyrus (BA 37,

TABLE I. Regional foci of rCBF changes: activations and deactivations (stimulation condition-rest)*

		Unimodal vestibular stimulation-rest (A vs. D)			Vestibular and visual stimulation-rest (C vs. D)			Unimodal visual stimulation-rest (B vs. D)		
Brain area	BA	x,y,z	*t*-value	vox.	x,y,z	*t*-value	vox.	x,y,z	*t*-value	vox.
VC	17–19	6,−90,−2	5.26	225[b]	**−8,−82,−2[a]**	**6.47**	**1130[b]**	**6,−84,16**	**13.27**	**12715[b]**
		−8,−94,−10[a]	4.59	225[b]	**2,−84,0[a]**	**4.43**	**1130[b]**	**−12,90,−2**	**6.48**	**12715[b]**
	18	−30,−70,−18	7.87	117	**−10,−62,2**	**4.56**	**42**			
					20,−70,6	**4.53**	**25**			
PCu	7	8,−86,44	7.60	516	**−6,−78,32**	**5.01**	**153[b]**	**−22,−76,30**	**10.37**	**12715[b]**
					4,−80,28	**5.00**	**153[b]**	**10,−78,30**	**10.48**	**12715[b]**
GTm/GOm	19/37	−42,−74,2	4.92	37	52,−74,−4	4.48	26	**50,−72,2**	**7.06**	**12715[b]**
								−52,−70,−4	**9.04**	**12715[b]**
PIVC		**40,−12,−2**	**8.86**	**1264[b]**	**38,−28,2**	**6.16**	**50**	−44,−26,8	4.32	12
		−48,−12,6	**5.11**	**107**						
PIVC/GTs	22	**−38,−32,14**	**5.29**	**93**				48,−20,4	5.24	1624[b]
GTs	38	**48,20,−28**	**5.16**	**20**				**30,20,−42**	**5.97**	**29**
GTs/GTm	21/22/38	**52,−36,14**	**7.21**	**1264[b]**						
	21/38/42							62,−12,−2	6.77	1624[b]
	21/22							−62,−8,−4	5.02	575
	21/38	−50,18,−30	4.48	9				−52,4,−22	5.25	33
GTm	37	−52,−50,−8	5.07	56						
	39	−42,−76,14	4.25	9	−40,−62,32	4.90	34	**58,−48,28**	**4.21**	**10**
	21	**66,−54,−10**	**4.77**	**4**						
LPi/GPoC	40							66,−14,20	8.14	1624[b]
LPi	40	**62,−48,34**	**4.22**	**3**	52,−66,40	4.72	40			
Th ant.-med.		**−6,−4,4**	**4.61**	**12**	**2,−6,8**	**5.03**	**21**			
Th post.-lat.		**−20,−20,2**	**5.07**	**13**						
GP								10,2,0	5.14	129
PCi	31	**6,−30,40**	4.16	12	−8,−34,34	4.25	2			
	23	**2,−4**,32	5.27	8	−16,0,40	4.79	9			
ACi	24/32	**−6,20,36**	5.08	85	**−2,10,54**	**4.36**	**11**			
ACi/GFd	10/11/32							−12,26,−14	7.34	4266[b]
								2,46,−12	5.20	4266[b]
GFm	46	**48,40,4**	**4.67**	**11**				36,28,−18	4.37	12
	8	**26,46,40**	**5.31**	**7**						
	10							32,52,−4	5.40	172
GFm/GFi	11/47	−48,50,−18	4.72	8						
GH		−30,−30,−6	4.95	12	**−20,−34,−12**	**4.59**	**2**	26,−16,−34	15.71	378
					12,−32,−12	**5.31**	**30**	−30,−8,−22	6.60	229
					−20,−12,−20	5.09	42			
					32,−24,−24	4.74	26			
					28,−12,−24	4.21	18			
		−44,−20,−24	4.87	12	40,−30,−16	4.52	8			
Cerebellum (hemispheres)		**−46,−68,−50**	**4.77**	**122**	**40,−46,−50**	**5.31**	**28**	**−62,−52,−30**	**5.14**	**31**
		−32,−56,−26	5.23	22	**−44,−70,−50**	**4.02**	**2**	**−38,−56,−34**	**4.53**	**10**
					−32,−32,−32	5.28	25	**52,−50,−42**	**4.06**	**9**
								−20,−40,−28	5.64	64

* Brain areas showing activations (bold letters) or deactivations during visual, vestibular, or combined stimulation vs. rest condition ($n = 13$, $P < 0.001$, uncorrected). Brodman areas (BA), MNI coordinates, number of voxels, and *t*-values for voxels showing maximum significance in each cluster are listed. ACi, anterior cingulate gyrus; d, medial; GF, frontal gyrus; GH, parahippocampal gyrus; GO, occipital gyrus; GP, Globus pallidus; GPoC, postcentral gyrus; GT, temporal gyrus; i, inferior; LP, parietal lobule; Lpc, paracentral lobule; m, middle; PCi, posterior cingulate gyrus; PCu, precuneus; PI, posterior insula; rCBF, regional cerebral blood flow; s, superior; Th, thalamus; VC, visual cortex.

[a] BA 17 and BA 18 only.

[b] This cluster is confluent with a cluster in another listed brain area; the voxel number represents the entire cluster.

BA 39), parahippocampal gyrus, and in the cerebellar hemisphere (Fig. 1; Table I).

Visual Motion Stimulation

Visual motion stimulation did not induce sensations of self-motion or nausea in any of the subjects. Group analysis showed the following signal changes.

Activations

Bilateral activations were elicited in the visual cortex (lingual, fusiform, and occipital gyri, BA 17–19), middle temporal/middle occipital gyri (BA 19/37), precuneus (BA 7), and in the cerebellar hemispheres. Right-sided activations occurred in the superior temporal (BA 38) and middle temporal (BA 39) gyri (Fig. 1; Table I). Significant activations in the visual cortex and middle temporal/middle occipital gyri (BA 19/37) were seen in the single-subject analyses of all subjects.

Deactivations appeared bilaterally in the posterior insula (long insular gyrus V) and retroinsular regions, extending to Heschl gyrus, in the superior temporal (BA 22/38) and middle temporal (BA 21) gyri. Further bilateral deactivations were seen in the anterior cingulate gyrus (BA 32), middle and medial frontal gyri (BA 10/11), and parahippocampal gyri. Additional deactivations of the right hemisphere appeared in the inferior parietal lobule/postcentral gyrus (BA 40), superior temporal gyrus (BA 42), middle frontal gyrus (BA 46), and in the globus pallidus. Left-sided deactivations occurred in the cerebellar hemisphere (Fig. 1; Table I).

Simultaneous Visual and Vestibular Stimulation

During this condition subjects did not experience rotatory vertigo or nausea. A caloric nystagmus was recorded during the scanning phase in 10 subjects. With eyes open, the slow-phase velocity of the caloric nystagmus was reduced by 69% compared to the caloric nystagmus with eyes closed in Condition A. The following signal changes were found in the group analysis.

Activations

Bilateral activations were seen in the visual cortex (BA 17/18, sparing BA 19), precuneus (BA 7), parahippocampal gyri, and cerebellar hemispheres. Unilateral activations of the right hemisphere were found in the posterior insula and retroinsular region (one cluster centered in the retroinsular region extending to Heschl gyrus and the long insular gyrus V) and in the antero-medial thalamus. A unilateral left-sided activation occurred in the anterior cingulate gyrus (BA 32) (Fig. 1; Table I).

Both typical visual and vestibular areas showed activations, but cluster sizes were smaller compared to unimodal stimulations. The number of activated voxels within the visual cortex areas decreased by a factor of about 10 from 12,715 voxels (BA 17–19, BA 7, BA 19/37) during visual stimulation to 1,350 voxels (BA 17, BA 18, BA 7) during simultaneous stimulation. Concurrently, the **t**-value decreased from 13.3 (unimodal vestibular) to 6.5 (bimodal). The number of activated voxels within the right posterior insula and retroinsular regions decreased from 1,264 voxels during vestibular stimulation to 50 voxels during the simultaneous condition, the *t*-value declined from 8.9 to 6.2. In the anterior cingulate gyrus the number of activated voxels declined from 85 voxels to 11 voxels; the *t*-value was reduced from 5.1 to 4.4. No brain areas showed signal changes only during bimodal stimulation.

Deactivations

Bilateral deactivations were seen in the parahippocampal gyri. Unilateral right-sided deactivations were located in the middle temporal/middle occipital gyri (BA 19/37) and inferior parietal lobule (BA 40). Left-sided deactivations were seen in the posterior cingulate (BA 23, BA 31) and middle temporal (BA 39) gyri, and in the hemisphere of the cerebellum. Deactivations in the inferior parietal lobule and posterior cingulate gyrus corresponded to areas, which were activated during unimodal vestibular stimulation (Fig. 1; Table I). Deactivations of the left middle temporal gyrus (BA 37, BA 39) decreased from 65 voxels (vestibular) to 34 voxels (combined). Deactivations of the parahippocampal region were also smaller with 607 voxels during visual stimulation and 94 voxels during simultaneous stimulation.

Unimodal Vs. Combined Stimulation

Statistical comparisons of the unimodal stimulation conditions vs. the combined condition were performed for the group. The vestibular minus combined comparison revealed clusters located bilaterally in the inferior parietal lobule (BA 40), superior temporal gyrus (BA 22), paracentral lobule (BA 7), anterior cingulate gyrus (BA 24/32), and middle frontal gyrus (BA 10/46 left and BA 10/47 right). Further clusters were

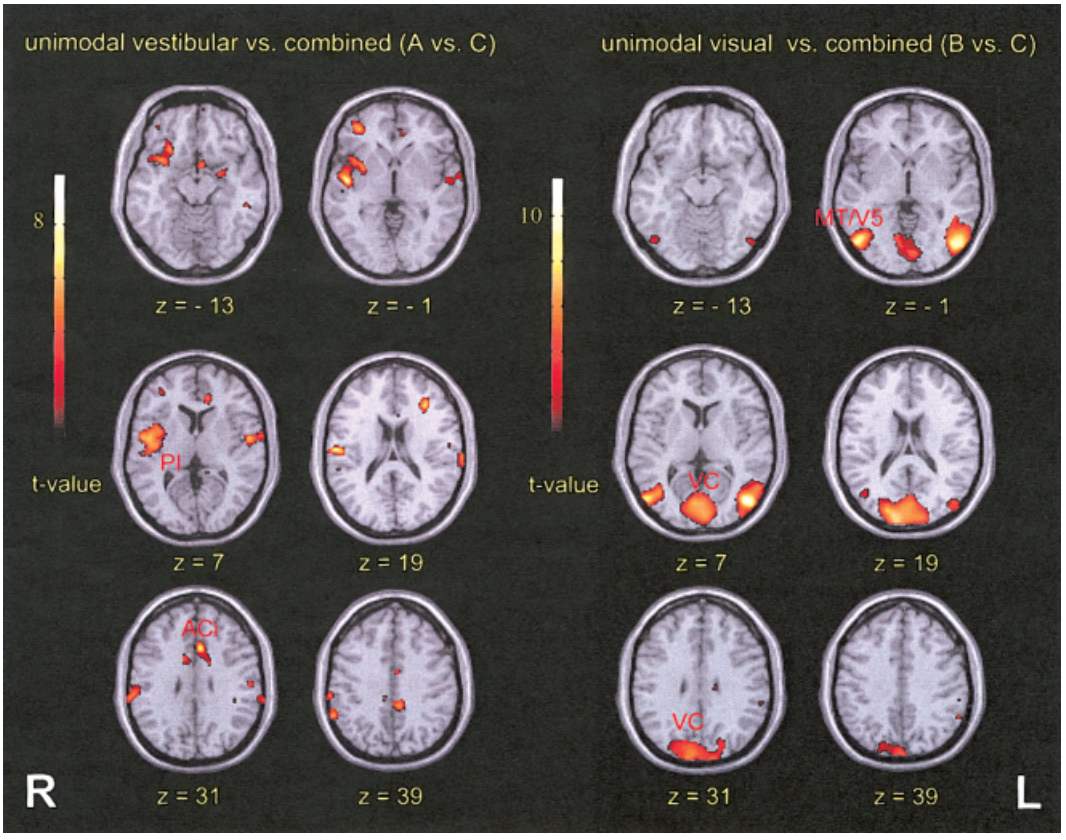

Figure 2.

Activation maps for the statistical comparison of unimodal vs. bimodal vestibular and visual stimulation ($n = 13$; $P < 0.001$; superimposed onto the MNI standard brain template). Left: vestibular vs. bimodal stimulation, right: visual vs. bimodal stimulation. ACi, anterior cingulate gyrus; PI, posterior insula; VC, visual cortex.

seen unilaterally in the right posterior insula, extending to the right inferior frontal (BA 47) and superior temporal (BA 22/38/42) gyri, as well as in the left inferior temporal (BA 20), left posterior cingulate (BA 23/31), and left parahippocampal gyri (Fig. 2; Table II).

In the visual minus combined comparison (group analysis) clusters were seen bilaterally in the visual cortex (BA 17–19), middle temporal/middle occipital gyri (BA 19/37), precuneus (BA 7), and inferior parietal lobule (BA 40). Additional clusters were located in the right superior parietal lobule (BA 7), left paracentral lobule (BA 7), left posterior cingulate gyrus (BA 23/31), and in the left cerebellar hemisphere (Fig. 2; Table II).

DISCUSSION

Unimodal vestibular and unimodal visual stimulation elicited typical patterns of rCBF changes, which confirmed findings of previous brain activation studies using vestibular stimulation [Bense et al., 2001; Bottini et al., 1994; Wenzel et al., 1996] and visual motion stimulation [Brandt et al., 1998, 2000; Bucher et al., 1997; Galati et al., 1999; Kleinschmidt et al., 1999; Previc et al., 2000]. Vestibular stimulation caused activations in temporo-parietal vestibular areas including the posterior insula and retroinsular regions as well as simultaneous deactivations of visual cortex areas. Visual motion stimulation induced activations of visual cortical regions including the motion-sensitive area MT/V5 in the middle temporal and middle occipital gyri and simultaneous deactivations of temporo-parietal vestibular areas. This finding supports the concept of an reciprocally inhibitory visual-vestibular interaction. During bimodal stimulation both sensory systems, visual and vestibular, were activated, but activation clusters were smaller and less significant than those elicited by unimodal stimulation. Most deactivations seen during unimodal stimulation in visual and vestibular brain areas were absent during

TABLE II. Regional foci of differential rCBF changes (unimodal-bimodal stimulation)*

		Unimodal visual-bimodal stimulation			Unimodal vestibular-bimodal stimulation		
Brain area	BA	Coordinates (x,y,z)	*t*-value	Number of voxels	Coordinates (x,y,z)	*t*-value	Number of voxels
VC	17–19	14,−96,26	8.39	4069[a]			
		−4,−94,14	7.39	4069[a]			
GTm/GOm	19/37	−48,−76,8	11.59	1630			
		50,−72,2	10.23	957			
PCu	7	−18,−46,58	4.71	19			
PI/GTs/LPi/GFi	22/38/42/40/47				28,24,−16	9.37	1887[a]
GTs	22				−56,−6,4	7.23	203
GTi	20				−68,−26,−28	6.27	30
LPi	40	−50,−52,40	4.34	9	64,−28,40	5.29	1887[a]
					60,−50,38	5.89	115
					−68,−34,26	6.23	214
					−62,−54,46	4.82	6
LPi/LPs	7/40	30,−54,56	5.23	110			
LPs/PCu	7	28,−78,52	4.86	67			
Lpc	7	−24,−28,54	7.81	89	0,−32,50	7.15	304
GFm	10/46				−34,30,20	7.47	116
GFm/GFi	10/47				36,44,−4	6.25	233
ACi	24/32				−8,18,28	9.81	213
					−14,38,8	4.89	55
					8,6,28	4.99	38
					−2,44,−6	5.34	60
PCi	23/31	−16,−18,32	4.20	5	−14,−40,10	4.96	10
GH	28/35				−26,−4,−18	5.72	95
Cerebellum (hemispheres)		−46,−74,−22	4.32	12			

* Brain areas showing activations in the unimodal vestibular minus bimodal comparison and unimodal visual minus bimodal comparison ($n = 13$, $P < 0.001$, uncorrected). Brodman areas (BA), MNI coordinates, number of voxels, and *t*-values for voxels showing maximum significance in each cluster are listed. ACi, anterior cingulate gyrus; d, medial; GF, frontal gyrus; GH, parahippocampal gyrus; GO, occipital gyrus; GP, Globus pallidus; GT, temporal gyrus; i, inferior; LP, parietal lobule; Lpc, paracentral lobule; m, middle; PCi, posterior cingulate gyrus; PCu, precuneus; PI, posterior insula; rCBF, regional cerebral blood flow; s, superior; Th, thalamus; VC, visual cortex.
[a] This cluster is confluent with a cluster in another listed brain area; the voxel number represents the entire cluster.

bimodal stimulation. In the following, we discuss the differential effects of unimodal and bimodal stimulation.

Activations During Unimodal Vestibular Stimulation

Activations seen in the contrast vestibular stimulation vs. rest (A vs. D) reflect both vestibular and ocular motor functions, because caloric nystagmus was present during the scanning period. We identified activations in the posterior insula and retroinsular regions (extending bilaterally to the superior temporal gyri), in the anterior insula, middle temporal, anterior cingulate, and middle frontal (BA 8, BA 46) gyri, in the inferior parietal lobule, and in the thalamus (both antero-medial and postero-lateral), which belong to a complex thalamo-cortical network involved in processing vestibular and ocular motor information.

Posterior insular and retroinsular activations represent the human homologue of the PIVC of the monkey, which is regarded as the core region within the multisensory cortical vestibular system [Grüsser et al., 1990a,b; Guldin and Grüsser, 1996]. The PIVC was delineated in electrophysiological studies in old and new world monkeys [Grüsser et al., 1990a,b] and cats [Jijiwa et al., 1991]. The authors found multisensory neurons, that responded not only to vestibular stimulation but also to somatosensory, visual, and optokinetic stimulation. Neurological patients with acute

ischemic lesions that involved the posterior insula and retroinsular areas had direction-specific tilts of the perceived visual vertical, indicating vestibular graviceptive dysfunction [Brandt et al., 1994]. Furthermore, the same area was found to be activated in functional imaging studies in humans using vestibular stimulation [galvanic: Bense et al., 2001; caloric: Bottini et al., 2001; Bucher et al., 1997]. Human brain activation studies also confirmed the multisensory input to this area, because visual motion stimulation caused a deactivation of the PIVC [Brandt et al., 1998]. Thus, the PIVC is involved in the processing of spatial orientation, self-motion perception, and the control of eye movements, e.g., during optokinetic nystagmus.

The extensions of the retroinsular activation clusters into the superior temporal gyri (BA 22) bilaterally and in the right middle temporal gyrus (BA 21) in our study were also seen during galvanic vestibular stimulation in fMRI [Bense et al., 2001]. They correspond to earlier reports by Penfield et al. [1957] on vertiginous sensations in patients induced by electrical cortical stimulation of the superior and middle temporal gyri. Additional activations in the inferior parietal lobule (BA 40) have also been described in human brain activation studies during galvanic vestibular stimulation [Bense et al., 2001] and correspond best to area 7b of the monkey [Faugier-Grimaud and Ventre, 1989]. This area and the anterior cingulate gyrus are also involved in ocular motor processing [cingulate gyrus: Paus et al., 1993; cingulate gyrus and BA 40: Dieterich et al., 1998].

The activation in the middle frontal gyrus (BA 8) seems too far anterior to correspond to the frontal eye field (FEF) as described in earlier fMRI studies [Beauchamp et al., 2001; Luna et al., 1998; Petit and Haxby, 1999]. The FEF may be involved in caloric-ally induced eye movements (vestibular nystagmus). Its involvement was also seen during saccades [Anderson et al., 1994; Sweeney et al., 1996], smooth pursuit eye movements [Petit et al., 1997; Petit and Haxby, 1999], and optokinetic nystagmus [Dieterich et al., 1998]. A separate activation in the middle frontal gyrus (BA 46) can be best attributed to the prefrontal cortex (PFC), which is involved in different ocular motor tasks [PET: Sweeney et al., 1996; fMRI: Müri et al., 1998] and in galvanic vestibular stimulation [Bense et al., 2001].

Activations in the anterior insula, the antero-medial, and the postero-lateral thalamus, that were seen in this PET study, agree with those seen during optokinetic nystagmus [Bucher et al., 1997; Dieterich et al., 1998] and during vestibular eye movements [Bense et al., 2001]. The simultaneous activations of the postero-lateral and paramedian thalamus and cortical ocular motor areas fit with the concept of an efferent motor loop between the basal ganglia, the thalamus, and (ocular) cortical areas according to Alexander et al. [1986] and thus may reflect an efference copy of ocular motor signals.

Activations During Unimodal Visual Stimulation

The contrast visual motion stimulation vs. rest (B vs. D) showed bilateral activations in occipital visual cortex areas. Activations of the temporo-parieto-occipital junction (BA 19/37) represent the human homologue of the motion-sensitive area MT/V5 of the monkey [Desimone and Ungerleider, 1986; Dubner and Zeki, 1971]. Several functional imaging studies in humans have shown that MT/V5 is involved in object-motion perception [Barton et al., 1996; Brandt et al., 2000; Previc et al., 2000; Zeki et al., 1991] and self-motion perception [Brandt et al., 1998; Cheng et al., 1995; de Jong et al., 1994]. Connections of MT/V5 to the vestibular system have been demonstrated in monkey studies, where vestibular input to visual-tracking neurons in MT/V5 [Thier and Erickson, 1992] and efferent pathways to the vestibular brainstem nuclei [Faugier-Grimaud and Ventre, 1989; Jeannerod, 1996] were described.

Deactivations During Unimodal Vestibular or Visual Stimulation

During unimodal vestibular stimulation those visual cortical areas were deactivated, which had been activated during visual motion stimulation (BA 17–19, BA 19/37). This confirms an earlier H_2O-15-PET study with caloric vestibular stimulation [Wenzel et al., 1996], where a decreased glucose metabolism in the visual cortex (BA 17–19) was observed in a patient with involuntary saccadic oscillations (opsoclonus).

In contrast, unimodal visual stimulation revealed a complex pattern of deactivations in cortical areas related to vestibular and ocular motor processing. This pattern included the PIVC, the superior and middle temporal gyri, the inferior parietal lobule, the middle frontal gyrus, and the anterior cingulate gyrus. Deactivation of the PIVC was also described during earlier brain activation studies on visually induced apparent self-motion perception [Brandt et al., 1998], visual motion stimulation [Brandt et al., 2000], and optokinetic nystagmus [Bense et al., 2000].

The functional significance of deactivations remains being discussed. It is now widely accepted that localized rCBF increases and BOLD signal increases are an

index of increased neuronal activity [Heeger et al., 2000; Jüptner and Weiller, 1995; Rauch et al., 1998; Rees et al., 2000] and correlate to local field potentials [Logothetis et al., 2001; Raichle, 2001]. Interpretations must take into account that inhibition is also energy-consuming [Ackerman et al., 1984], so that activations can therefore be due either to neuronal excitation or to inhibition. Localized deactivations may be as important for brain function as activations. Task-induced BOLD signal decreases most likely reflect functional deactivation [Votaw et al., 1999]. Although earlier reports found disparities in the comparison of negative BOLD signal changes seen with fMRI techniques and rCBF decreases seen with PET [Sadato et al., 1998; Schlösser et al., 1998], recent studies emphasize the congruity of deactivations in PET and fMRI elicited by the same paradigm [Bense et al., 2000; Votaw et al., 1999].

Simultaneous Visual-Vestibular Stimulation

The novel approach of the current study was to present both sensory stimuli, visual and vestibular, simultaneously. When simulating natural motion stimuli in PET and fMRI, the investigator is faced with several methodological restrictions. In particular, it is not possible to apply a natural vestibular stimulus, as it occurs during passive or active head movement. Thus, the visual-vestibular stimulation used in the study was experimental with unknown ratio of the stimuli strengths. It is important to test the combined stimulation, because it comes closer to natural locomotion, which inevitably involves multisensory input. Bimodal stimulation yielded characteristic qualitative and quantitative changes.

Activations during bimodal stimulation were smaller and less significant than during unimodal stimulation, as illustrated by a decrease of the number of activated voxels per cluster and of *t*-values. The cluster sizes decreased by a factor of 26 for the right posterior insula and retroinsular regions, by a factor of 10 for the primary visual cortex, and by a factor of 7 for the anterior cingulate gyrus. These differences were particularly evident in the subtraction analyses (unimodal vs. bimodal stimulation, Fig. 2). Some activations, e.g., in the inferior parietal lobule (BA 40) and in the middle frontal gyrus (BA 46, BA 8), did not occur during simultaneous stimulation. Deactivations almost completely disappeared; the "largest" cluster, located in the parahippocampal gyrus, consisted of only 42 voxels.

It must be noted that the presentation of a visual stimulus after caloric vestibular stimulation partially suppresses the vestibular nystagmus. This was reflected by a reduction of the slow-phase velocity of the vestibular nystagmus with the eyes open. The differential effects of the conditions eyes open vs. eyes closed on eye movements may therefore contribute to the rCBF changes observed. Moreover, it should be considered that the planes of motion stimulation could not be aligned due to methodological restrictions (vestibular stimulation: horizontal canal plane; visual stimulation: roll plane).

It might be interesting to use galvanic instead of caloric vestibular stimulation in a similar set-up. We have, however, made the experience in several fMRI studies that galvanic stimulation is a much weaker vestibular stimulus, and it induces the sensation of tilt rather than of continuous motion. Moreover, it is difficult to apply galvanic stimulation for a whole PET scanning period, because it evokes the sensation of pain and sometimes even damages the skin.

In conclusion, our findings of unimodal and bimodal stimulation are compatible with a reciprocally inhibitory visual-vestibular interaction. The inhibitory sensory interaction during bimodal stimulation could be the reason, why activation clusters of both sensory areas were smaller than during unimodal stimulation. Simultaneous stimulation of two sensory systems may lead to reciprocal distraction of perceptual sensitivity. It is reasonable that attentional shifts reduce activation or cause deactivation in cortical areas representing other sensory modalities. In PET studies using visual attentional paradigms deactivations in auditory cortex areas were seen and explained by selective attention [Haxby et al., 1994; Kawashima et al., 1999].

An inhibitory visual-vestibular and vestibulo-visual interaction has functional significance: the sensorial weight can be shifted from one modality to the other. The perception of self-motion can be dominated either by vestibular input, provided mainly by head acceleration, or by visual input during passive locomotion at a constant velocity with the head still, e.g., in a train, depending on the prevailing mode of stimulation. This mechanism makes it possible to relate the dominant perception of self-motion or orientation to the actual input of one of the two modalities and thus to avoid perceptual ambiguity [Brandt and Dieterich, 1999].

ACKNOWLEDGMENT

We thank J. Benson for critically reading the manuscript.

REFERENCES

Ackermann RF, Finch DM, Babb TL, Engel J Jr (1984): Increased glucose metabolism during long-duration recurrent inhibition of hippocampal pyramidal cells. J Neurosci 4:251–264.

Alexander GE, DeLong MR, Strick PL (1986): Parallel organization of functionally segregated circuits linking basal ganglia and cortex. Annu Rev Neurosci 9:357–381.

Anderson TJ, Jenkins IH, Brooks DJ, Hawken MB, Frackowiak RS, Kennard C (1994): Cortical control of saccades and fixation in man. A PET study. Brain 117:1073–1084.

Barton JJ, Simpson T, Kiriakopoulos E, Stewart C, Crawley A, Guthrie B, Wood M, Mikulis D (1996): Functional MRI of lateral occipitotemporal cortex during pursuit and motion perception. Ann Neurol 40:387–398.

Beauchamp MS, Petit L, Ellmore TM, Ingeholm J, Haxby JV (2001): A parametric fMRI study of overt and covert shifts of visuospatial attention. NeuroImage 14:310–321.

Bense S, Stephan T, Yousry TA, Schwaiger M, Dieterich M, Brandt T (2000): FMRI and PET during optokinetic stimulation: comparison of activation and deactivation patterns. J Neurol 247:163.

Bense S, Stephan T, Yousry TA, Brandt T, Dieterich M (2001): Multisensory cortical signal increases and decreases during vestibular galvanic stimulation (fMRI). J Neurophysiol 85:886–899.

Bottini G, Sterzi R, Paulesu E, Vallar G, Cappa SF, Erminio F, Passingham RE, Frith CD, Frackowiak RS (1994): Identification of the central vestibular projections in man: a positron emission tomography activation study. Exp Brain Res 99:164–169.

Bottini G, Karnath HO, Vallar G, Sterzi R, Frith CD, Frackowiak RS, Paulesu E (2001): Cerebral representations for egocentric space: functional-anatomical evidence from caloric vestibular stimulation and neck vibration. Brain 124:1182–1196.

Brandt T, Dieterich M, Danek A (1994): Vestibular cortex lesions affect the perception of verticality. Ann Neurol 35:403–412.

Brandt T, Bartenstein P, Janek A, Dieterich M (1998): Reciprocal inhibitory visual-vestibular interaction. Visual motion stimulation deactivates the parieto-insular vestibular cortex. Brain 121: 1749–1758.

Brandt T, Dieterich M (1999): The vestibular cortex. Its locations, functions, and disorders. Ann NY Acad Sci 871:293–312.

Brandt T, Stephan T, Bense S, Yousry TA, Dieterich M (2000): Hemifield visual motion stimulation: an example of interhemispheric crosstalk. NeuroReport 11:2803–2809.

Bucher SF, Dieterich M, Seelos KC, Brandt T (1997): Sensorimotor cerebral activation during optokinetic nystagmus. A functional MRI study. Neurology 49:1370–1377.

Bucher SF, Dieterich M, Wiesmann M, Weiss A, Zink R, Yousry TA, Brandt T (1998): Cerebral functional magnetic resonance imaging of vestibular, auditory, and nociceptive areas during galvanic stimulation. Ann Neurol 44:120–125.

Cheng K, Fujita H, Kanno I, Miura S, Tanaka K (1995): Human cortical regions activated by wide-field visual motion: an $H_2(15)O$ PET study. J Neurophysiol 74:413–427.

de Jong BM, Shipp S, Skidmore B, Frackowiak RS, Zeki S (1994): The cerebral activity related to the visual perception of forward motion in depth. Brain 117:1039–1054.

Desimone R, Ungerleider LG (1986): Multiple visual areas in the caudal superior temporal sulcus of the macaque. J Comp Neurol 248:164–189.

Dieterich M, Bucher SF, Seelos KC, Brandt T (1998): Horizontal or vertical optokinetic stimulation activates visual motion-sensitive, ocular motor and vestibular cortex areas with right hemispheric dominance. An fMRI study. Brain 121:1479–1495.

Dieterich M, Bense S, Brandt T, Schwaiger M, Bartenstein P (1999): Dominance of the non-dominant hemisphere for processing vestibular information (a PET study). NeuroImage 9:S499.

Dubner R, Zeki SM (1971): Response properties and receptive fields of cells in an anatomically defined region of the superior temporal sulcus in the monkey. Brain Res 35:528–532.

Faugier-Grimaud S, Ventre J (1989): Anatomic connections of inferior parietal cortex (area 7) with subcortical structures related to vestibulo-ocular function in a monkey (*Macaca fascicularis*). J Comp Neurol 280:1–14.

Frison L, Pocock S (1992): Repeated measures in clinical trials: analysis using mean summary statistics and its implications for design. Stat Med 11:1685–1704.

Friston KJ, Frith CD, Liddle PF, Dolan RJ, Lammertsma AA, Frackowiak RS (1990): The relationship between global and local changes in PET scans. J Cereb Blood Flow Metab 10:458–466.

Friston K, Holmes AP, Worsley K, Poline J-B, Frith C, Frackowiak RSJ (1995a): Statistical parametric maps in functional imaging: a general linear approach. Hum Brain Mapp 2:189–210.

Friston K, Ashburner J, Frith CD, Poline J-B, Heather JD, Frackowiak RSJ (1995b): Spatial registration and normalization of images. Hum Brain Mapp 2:165–189.

Galati G, Pappata S, Pantano P, Lenzi GL, Samson Y, Pizzamiglio L (1999): Cortical control of optokinetic nystagmus in humans: a positron emission tomography study. Exp Brain Res 126:149–159.

Grüsser OJ, Pause M, Schreiter U (1990a): Localization and responses of neurones in the parieto-insular vestibular cortex of awake monkeys (*Macaca fascicularis*). J Physiol 430:537–557.

Grüsser OJ, Pause M, Schreiter U (1990b): Vestibular neurones in the parieto-insular cortex of monkeys (*Macaca fascicularis*): visual and neck receptor responses. J Physiol 430:559–583.

Guldin W, Grüsser OJ (1996): The anatomy of the vestibular cortices of primates. In: Collard M, Jeannerod M, Christen Y, editors. Le cortex vestibulaire. Paris: Ipsen. p 17–26.

Haxby JV, Horwitz B, Ungerleider LG, Maisog JM, Pietrini P, Grady CL (1994): The functional organization of human extrastriate cortex: a PET-rCBF study of selective attention to faces and locations. J Neurosci 14:6336–6353.

Heeger DJ, Huk AC, Geisler WS, Albrecht DG (2000): Spikes vs. BOLD: what does neuroimaging tell us about neuronal activity? Nat Neurosci 3:631–633.

Jeannerod M (1996): Vestibular cortex. A network for directional coding of behavior. In: Collard M, Jeannerod M, Christen Y, editors. Le Cortex vestibulaire. Paris: Ipsen. p 5–15.

Jijiwa H, Kawaguchi T, Watanabe S, Miyata H (1991): Cortical projections of otolith organs in the cat. Acta Otolaryngol 481(Suppl):69–72.

Jüptner M, Weiller C (1995): Review: does measurement of regional cerebral blood flow reflect synaptic activity? Implications for PET and fMRI. NeuroImage 2:148–156.

Kawashima R, Imaizumi S, Mori K, Okada K, Goto R, Kiritani S, Ogawa A, Fukuda H (1999): Selective visual and auditory attention toward utterances-a PET study. NeuroImage 10:209–215.

Kleinschmidt A, Thilo KV, Büchel C, Gresty MA, Bronstein AM, Frackowiak RSJ (1999): Cerebral processing of visual-motion as object- or self-motion. NeuroImage 9:6.

Lobel E, Kleine JF, Bihan DL, Leroy-Willig A, Berthoz A (1998): Functional MRI of galvanic vestibular stimulation. J Neurophysiol 80:2699–2709.

Logothetis NK, Pauls J, Augath M, Trinath T, Oeltermann A (2001): Neurophysiological investigation of the basis of the fMRI signal. Nature 412:150–157.

Luna B, Thulborn KR, Strojwas MH, McCurtain BJ, Berman RA, Genovese CR, Sweeney JA (1998): Dorsal cortical regions subserving visually guided saccades in humans: an fMRI study. Cereb Cortex 8:40–47.

Müri RM, Heid O, Nirkko AC, Ozdoba C, Felblinger J, Schroth G, Hess CW (1998): Functional organization of saccades and antisaccades in the frontal lobe in humans: a study with echo planar functional magnetic resonance imaging. J Neurol Neurosurg Psychiatry 65:374–377.

Naidich TP, Brightbill TC (1996): Systems for localizing frontoparietal gyri and sulci on axial CT and MRI. Int J Neuroradiol 2:313–338.

Oldfield RC (1971): The assessment and analysis of handedness: the Edinburgh inventory. Neuropsychologia 9:97–113.

Paus T, Petrides M, Evans AC, Meyer E (1993): Role of the human anterior cingulate cortex in the control of oculomotor, manual, and speech responses: a positron emission tomography study. J Neurophysiol 70:453–469.

Penfield W (1957): Vestibular sensation and the cerebral cortex. Ann Otol 66:691–714.

Petit L, Clark VP, Ingeholm J, Haxby JV (1997): Dissociation of saccade-related and pursuit-related activation in human frontal eye fields as revealed by fMRI. J Neurophysiol 77:3386–3390.

Petit L, Haxby JV (1999): Functional anatomy of pursuit eye movements in humans as revealed by fMRI. J Neurophysiol 82:463–471.

Previc FH, Liotti M, Blakemore C, Beer J, Fox P (2000): Functional imaging of brain areas involved in the processing of coherent and incoherent wide field-of-view visual motion. Exp Brain Res 131:393–405.

Raichle ME (2001): Cognitive neuroscience. Bold insights. Nature 412:150–157.

Rauch SL, Whalen PJ, Curran T, McInerney S, Heckers S, Savage CR (1998): Thalamic deactivation during early implicit sequence learning: a functional MRI study. NeuroReport 9:865–870.

Rees G, Friston K, Koch C (2000): A direct quantitative relationship between the functional properties of human and macaque V5. Nat Neurosci 3:716–723.

Sadato N, Yonekura Y, Yamada H, Nakamura S, Waki A, Ishii Y (1998): Activation patterns of covert word generation detected by fMRI: comparison with 3D PET. J Comput Assist Tomogr 22:945–952.

Salmaso D, Longoni AM (1985): Problems in the assessment of hand preference. Cortex 21:533–549.

Schlösser R, Hutchinson M, Joseffer S, Rusinek H, Saarimaki A, Stevenson J, Dewey SL, Brodie JD (1998): Functional magnetic resonance imaging of human brain activity in a verbal fluency task. J Neurol Neurosurg Psychiatry 64:492–498.

Stephan KM, Schüller M, Höflich P, Knorr U, Binkofski F, Seitz RJ (1997): Normalization in Talairach space: variability of reference coordinates. NeuroImage 5:416.

Sweeney JA, Mintun MA, Kwee S, Wiseman MB, Brown DL, Rosenberg DR, Carl JR (1996): Positron emission tomography study of voluntary saccadic eye movements and spatial working memory. J Neurophysiol 75:454–468.

Talairach J, Tournoux P (1988): Co-planar stereotactic atlas of the human brain. Stuttgart: Thieme Verlag.

Thier P, Erickson RG (1992): Vestibular input to visual-tracking neurons in area MST of awake rhesus monkeys. Ann NY Acad Sci 656:960–963.

Votaw JR, Faber TL, Popp CA, Henry TR, Trudeau JD, Woodard JL, Mao H, Hoffman JM, Song AW (1999): A confrontational naming task produces congruent increases and decreases in PET and fMRI. NeuroImage 10:347–356.

Wenzel R, Bartenstein P, Dieterich M, Danek A, Weindl A, Minoshima S, Ziegler S, Schwaiger M, Brandt T (1996): Deactivation of human visual cortex during involuntary ocular oscillations. A PET activation study. Brain 119:101–110.

Woods RP (1996): Modeling for intergroup comparisons of imaging data. NeuroImage 4:84–94.

Worsley KJ, Friston KJ (1995): Analysis of fMRI time-series revisited-again. NeuroImage 2:173–181.

Yousry TA, Fesl G, Büttner A, Noachtar S, Schmid DU, Peraud A, Büttner A, Winkler P (1997): Heschl gyrus: anatomic description and methods of identification in MRI. Int J Neuroradiol 3:2–12.

Zeki S, Watson JD, Lueck CJ, Friston KJ, Kennard C, Frackowiak RS (1991): A direct demonstration of functional specialization in human visual cortex. J Neurosci 11:641–649.